Available online at www.sciencedirect.com

ScienceDirect

journal homepage: www.elsevier.com/locate/he

Hydrogen sensing by RGB investigation of gasochromic coloration of MoO_3/Pd-coated polyester fabrics

Z. Masoumi Dehaghi, M. Ranjbar, M. Torabi Goodarzi*

Department of Physics, Isfahan University of Technology, Isfahan, 8415683111, Iran

HIGHLIGHTS

- Sputter deposited MoO_3/Pd on polyester were explored for gasochromic hydrogen sensing.
- RGB color sensor module was used for acquiring color changes.
- RGB data showed a linear behavior with respect to hydrogen concentration (250–10,000 ppm).
- Significant correlation was found between RGB readout and absorption spectra.
- Coloration time, reversibility and reproducibility were also evaluated by RGB data.

GRAPHICAL ABSTRACT

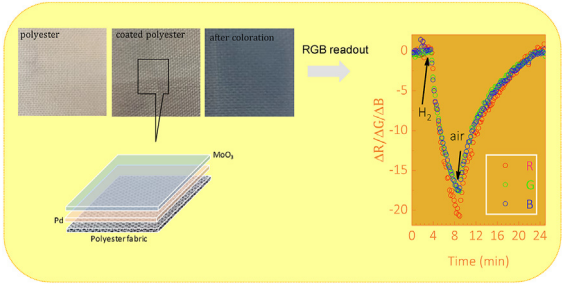

ARTICLE INFO

Article history:
Received 25 May 2021
Received in revised form
6 September 2021
Accepted 23 September 2021
Available online 10 October 2021

Keywords:
Hydrogen sensing
Gasochromic
MoO_3
Polyester fabrics
Sputtering
RGB color sensor

ABSTRACT

Recently, colorimetric sensors capable of detecting explosive and toxic molecules have attracted much attention for applications in health and environmental monitoring. Here, we demonstrate the detection of hydrogen gas using gasochromic fabrics and evaluate their performance with a commercial RGB color sensor module. For this purpose, first a thin Pd film was sputter deposited onto the polyester fabric and then amorphous MoO_3 films (several microns) were deposited by RF reactive magnetrons in various O_2/Ar ratios (from 2.5 to 12.5 O_2). Field emission scanning electron microscope (FESEM) identified the morphological changes of the surface at each coating step and showed that the fibrous structure of the fabrics was preserved after coating of the films, which is suitable for better gas adsorption. Exposure to hydrogen caused the obtained MoO_3/Pd/polyester samples to turn blue-gray at room temperature and the UV–Vis spectra showed an increase in optical absorption. Their sensitivity was evaluated in the presence of different H_2 concentrations from 250 to 10,000 ppm by recording the time variation of color difference (RGB Euclidean distance). A significant correlation was found between absorption spectrum and RGB analysis with respect to oxygen content. The color variation showed a linear behavior with respect to hydrogen concentration for all samples. Response and recovery times,

* *Corresponding author.*
E-mail address: ranjbar@iut.ac.ir (M. Ranjbar).
https://doi.org/10.1016/j.ijhydene.2021.09.195

reversibility and reproducibility in the presence of hydrogen gas were also evaluated using the RGB readout data. Overall, the RGB module optimally depicts the sensing characteristics of the gasochromic fabrics in terms of reversibility, sensitivity and reproducibility, which may contribute to their commercial development.

Introduction

In recent years, hydrogen has attracted much attention as a renewable and clean energy source [1]. It is also known as a cooling gas in power plants [2] and as an effective reducing agent in various industries such as semiconductor processing [3], fossil fuel decarbonization [4] and metallurgy [5]. However, hydrogen is a colorless, tasteless and odorless gas. Due to its low explosion threshold but high combustion energy, if the concentration of hydrogen exceeds the explosion limit of 4% molar fraction in air, it can have an explosive manner leading to huge damage especially when it is excessively accumulated indoors. Therefore, rapid and safe detection of hydrogen leakage at low concentrations in an explosion hazard environment is crucial.

So far, the research on the hydrogen detecting topic focuses mainly on the electrical and electrochemical [6–9] sensing platforms, many of which require high temperatures for good performance but have been successfully developed in electronic devices. In addition, the optical read-out hydrogen sensors based on optical fibers [10,11], colorimetric [12] and plasmonic nanomaterials [13] can provide desirable reliability and are explosion-proof due to low power electrical consumption. However, commercialization of these techniques are limited by the high cost of and difficulties in miniaturization of fiber-optics equipment, spectrophotometers and image processing devices. Fortunately, advances in the low-cost optoelectronic components promises the development and commercialization of chromic processes. RGB color sensor modules like TCS3200 are small, cost-effective options in which light is divided into a set of colors: primarily red (R), green (G), and blue (B). RGB color sensors are vastly used in different area such as agriculture, medicine and robotics [14,15]. In particular, RGB data can also be recorded and analyzed by mobile applications. There are also reports on RGB color sensors usage for chemical- and bio-sensing which has recently received more attention. For example, Lee. et al. [16] used commercial RGB sensors for rapid (~10 s) detection of low ppm concentration of hydrogen cyanide gas by using immobilized monocyanocobinamide. Fatoni et al. [17]. Successfully used RGB color sensor for colorimetric detection of hydrogen peroxide by color change as a result of reaction with titanium oxysulfate. Despite many reports on hydrogen colorimetric sensing, as far as we know, no report exists on hydrogen sensing by RGB module or analysis.

Transition metal oxides, as a major colorimetric and hydrogen sensitive martial class, can change their optical properties over a wide range of wavelengths when exposed to dilute hydrogen gas, known as gasochromic effect [18–20] because it has good reversibility. According to literature, tungsten oxide has often had better gasochromic properties than molybdenum oxide in terms of reversibility. However, molybdenum oxide gives more color depth, but its main problem so far has been its irreversibility compared to tungsten oxide. The main factor that has made molybdenum oxide less noticeable for gas chromic applications is perhaps its poor reversibility. Recently, efforts have been made to make this oxide reversible. For example, in the presence of the Pt/Ni/Pt catalyst layer, reversibility has been shown to improve [21]. MoO_3 provides more color depth and at the same time it has more color stability, and has been recently studied for eye-readable hydrogen sensor [22–24]. The molybdenum oxide absorption band in the reduced state after the gasochromic process is located at shorter wavelengths close to the visible area compared to WO_3, which makes it a better candidate for naked eye sensors in terms of sensitivity [25].

Although there are many reports on the gasochromic properties of transition metal oxides, most have studied the existing principles using optical transmission or reflection spectra and have relied less on the development of inexpensive measurement methods. In addition, RGB optical sensing techniques are based on reflection mode and are better compatible with wearable technologies [26,27], which essentially require extensive research on yarns and fabrics activated with gas-sensitive coatings. Fabrics, in addition to providing a sufficient surface to absorb gas, are flexible, foldable, and lightweight, and are available in a variety of materials, textures, colors, and transparency and have recently been used as colorimetric sensors [12,28]. Therefore, the development of flexible gasochromic fabrics can be a good candidate for integration with low-cost RGB sensors.

To date, MoO_3 films have been deposited by different methods on different substrates [29–34], which have divers properties and capabilities. Among them, magnetron sputtering provides fast deposition, good film and substrate adhesion, high film purity and uniformity, repeatability and easy to industrialize for large scales [35].

Palladium is commonly used as a selective hydrogen catalyst to promote gas dissociation in hydrogenation processes are extremely important in terms of excellent and stable catalytic properties at room temperature, which is doped into or deposited as a top layer on a hydrogen-sensitive material [36–39]. Hydrogen dissolves well at room temperature in palladium and diffuses into and react with the adjacent materials via a spillover process. In recent years, we have

prepared and studied hydrogen sensors based on gasochromic MoO_3 and WO_3 [40–44]. For example, we have fabricated flexible tungsten oxide nanofabrics by electrospining and studied their gasochromic properties to detect hydrogen. In the electrospinning method, controlling the composition of the solution as well as strengthening the fabrics was challenging [44]. On the other hand, we have shown that flexible and sensitive resistive hydrogen sensors can be produced via sputtering of palladium layers on filtration paper [45] or electrospan fabrics [46]. Therefore, one objective of this new work is to develop gasochromic fabrics with sputtered Pd and MoO_3 layers on polyester as a flexible substrate. By this way, the fibrous nature of the substrate allows gas to penetrate from both sides. Another objective is to use RGB data to track changes in the appearance of samples by coupling the fabrics into the commercial RGB color sensor. We observed that if the molybdenum oxide is deposited prior to palladium (Pd/MoO_3/polyester), the sputtering plasma from the palladium target leads to deep darkening of molybdenum oxide layer. Therefore, we choose the MoO_3/Pd/polyester configuration and fortunately observed the desired sensing properties. Formation of a thin PdO layer is possible in sputtering deposition due presence of partial oxygen pressure in the post-deposition of MoO_3 layer. But this oxide layer can be reduced in the presence of hydrogen gas and affect the catalytic efficiency of palladium. In addition, we believe that due to the layered nature of MoO3 crystal structure, hydrogen molecules can penetrate easily and riches the Pd layer through the van der Waals layers. Then the dissociated ions diffuse into the gasochromic layer. For gasochromic hydrogen sensing investigations, the created layers were exposed to various hydrogen concentrations at room temperature. This study also examines the role of oxygen percent in sputtering.

Experimental

Deposition of Pd and MoO_3 films

In this paper, the untreated polyester fabrics with a density of 5% were used as the substrate. Firstly, a thin layer of palladium with 10 nm thickness was pre-deposited on fabrics by DC magnetron sputtering using a palladium target (99.99% purity) In the deposition of Pd layer, a 40 W DC power was applied. The chamber base pressure was 5×10^{-5} mbar and the working pressure was set to 6×10^{-2} mbar. The target to substrate distance was 10 cm and deposition time was 20 s. Thereafter, MoO_3 thin films were deposited by RF reactive magnetron sputtering using a MoO_3 target (purity 99.99%) with 100 W RF power. The O_2/Ar ratio was considered as the variable parameter in the deposition of gasochromic layers. The chamber evacuated to base pressure of 5×10^{-5} mbar before deposition process, then increased to 5×10^{-2} mbar by insertion of O_2/Ar mixture. Argon and oxygen gases were regulated separately by different mass flow controllers (MFCs). Considering different oxygen percent, five different samples were prepared, which were named as $S_{2.5}$, S_5, $S_{7.5}$, S_{10} and $S_{12.5}$ where the subscript shows the oxygen percentage. The total deposition time for MoO_3 was 30 min, and the target to substrate distance was 7.5 cm.

Characterizations

The surface morphology of the samples was investigated by field emission scanning electron microscopes model QUANTA FEG450. An Asenware AW-XDM300 GIXRD system (CuKα $\lambda = 1.5405$ Å) was used to study the crystallinity of fabricated layers. To quantitatively compare the color variation of the samples, the reflectance spectra of the samples acquired in the visible wavelength range (400–700 nm) by Spectra Flash 600 datacolor spectrophotometer.

For investigating the dynamic gasochromic coloration, samples were mounted inside a small test chamber with inlet and outlet valves (Fig. 1(a)). Different concentrations hydrogen (250–10000 ppm) were prepared by mixing H_2 and Ar using MFCs with total flow rate of 2 l/min. The coloration of coated fabrics samples was quantitatively measured using RGB analysis by a TCS3200 RGB color sensor module equipped with four white LEDs, and recorded into a PC by an Ardunio Uno microcontroller platform. The coloration process was performed by 5 min hydrogen exposure and the bleaching process was performed by introduction of the ambient air.

Result and discussion

In order to investigate the optical hydrogen sensing properties of the gasochromic fabrics using RGB module in this study, the samples were mounted in the sample holder of the sensing box (Fig. 1(a)) and they were exposed alternatively to hydrogen gas or air. We turned-on the white LED light source of the module to obtain reflection RGB data. All the hydrogenation processes were performed at room temperature. The initial gray color of the gasochromic fabrics turns blue-gray when exposed to hydrogen gas and the values of ΔR, ΔG and ΔB gradually decrease with hydrogen exposing time as shown typically in Fig. 1(b) for sample $S_{7.5}$ in the presence of 3000 ppm H_2. The decrease in R, G and B data is in agreement with appearance of the blue-gray color. K. You et al. [25] have reported color change from white to blue-gray color in their investigation on Pd-modified MoO_3 nanofibers. Ref [22] reported similar observation of Pd-modified MoO_3 nanowire labels. From Fig. 1(b), after the replacement of hydrogen by air, all RGB data return to their original values over a longer period of time.

FESEM and X-ray diffraction

The surface morphology of the blank polyester fabric and polyesters fabrics coated with gasochromic films including samples $S_{2.5}$ to $S_{12.5}$ were observed under FESEM (Fig. S1). Fig. 2 left panel shows some selective images at different magnification scales of a polyester coated with Pd layer only and a representative gasochromic sample (S_{10}). The fibrous structure of the blank fabric is woven of warp and weft with monofibers of about 10 μm thick (see arrows). They have no interconnected morphology due of gaps between the individual fabrics. The fabrics show also no significant change in diameter due to the Pd layer coating, but they show a distinct deformation of diameter from 10 up to approximately 20 μm due to the molybdenum oxide coating, estimating thickness of

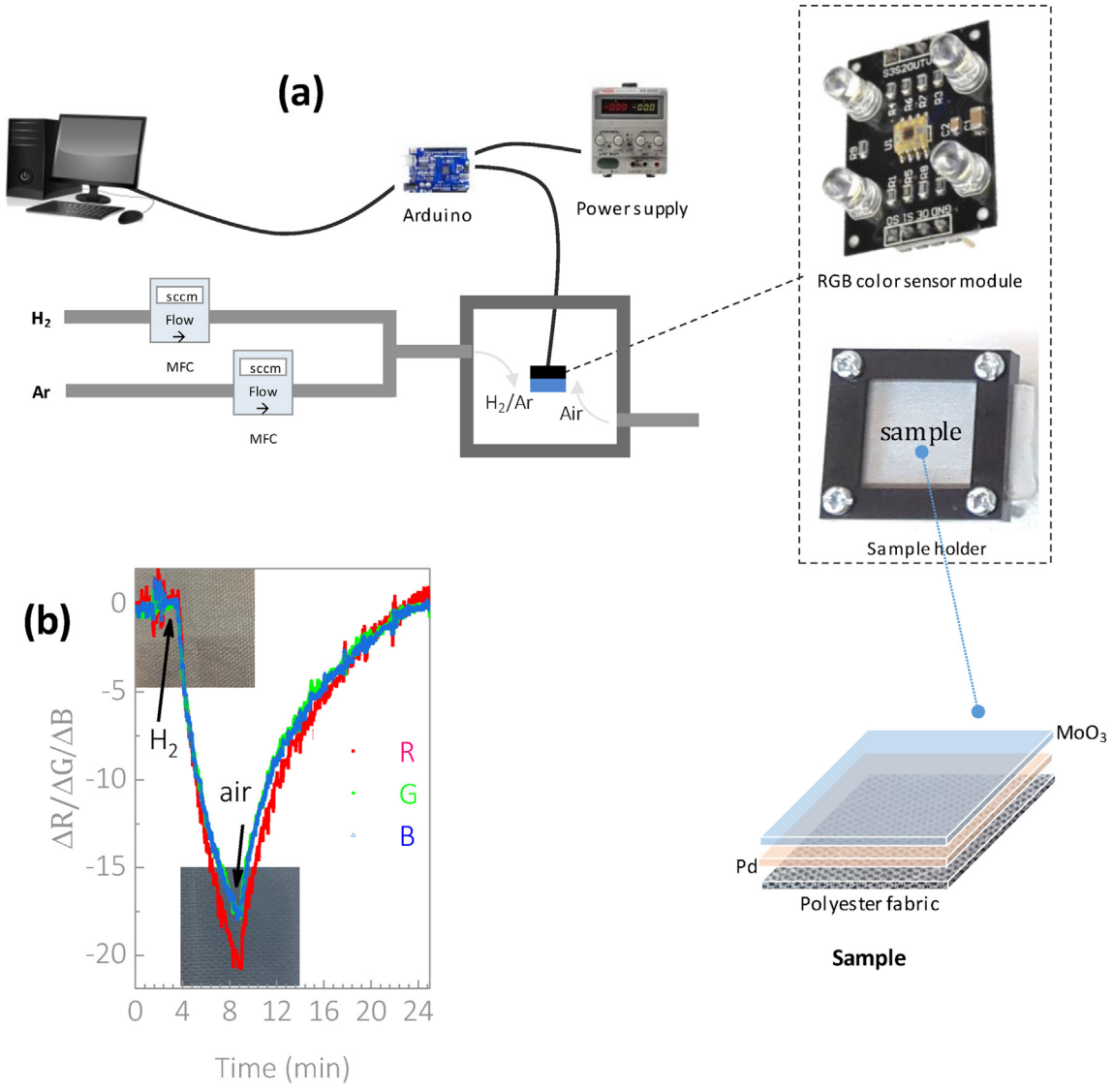

Fig. 1 – (a) Schematic representation of the experimental setup used to investigate the gasochromic performance of MoO_3/Pd/Polyester samples with RGB color sensor module. (b) ΔR, ΔG and ΔB values after exposing sample $S_{7.5}$–3000 ppm H_2. All of the RGB values decrease gradually with exposure time and recover to the initial background when hydrogen is replaced with air. (For interpretation of the references to color in this figure legend, the reader is referred to the Web version of this article.)

MoO_3 layers in order of several micrometers. As the FESEM images of higher magnifications show, the single fabrics of blank polyester have relatively rough surfaces and palladium coating makes their surfaces much smoother. However, due to the deposition of the MoO_3 layer, the surface of the individual fabrics has become significantly rougher than that of the blank polyester, and the formation of the MoO_3 layer can be understandable from the formation of cracks along the connection of fabrics (shown by arrows in the FESEM image). Formation of cracks in the MoO_3 films can be related to stretching of the surface during or after the coating process. In addition, the fabrics do not stick tightly together thus the deposited layers do not completely fill their spacing gaps, which preserves the open structure of the fabrics, allowing high absorption of hydrogen and desirable sensing.

Fig. 2 right panel shows grazing incidence X-ray diffraction (GIXRD) patterns of all $S_{2.5}$-$S_{12.5}$ samples. The three observed peaks in the range of 15–30° refer to diffractions along the (100), (002) and (101) directions of the quasi-crystalline polyester phase [47]. There are no visible diffraction peaks related to MoO_3 or Pd, suggesting that MoO_3 is amorphous and the palladium layer is very thin. Although crystalline MoO_3 films have been vastly reported in resistive-type gas sensors they often operate at high working temperature [48]. Amorphous MoO_3, however, is desirable for gasochromic switching even at room temperature [49,50].

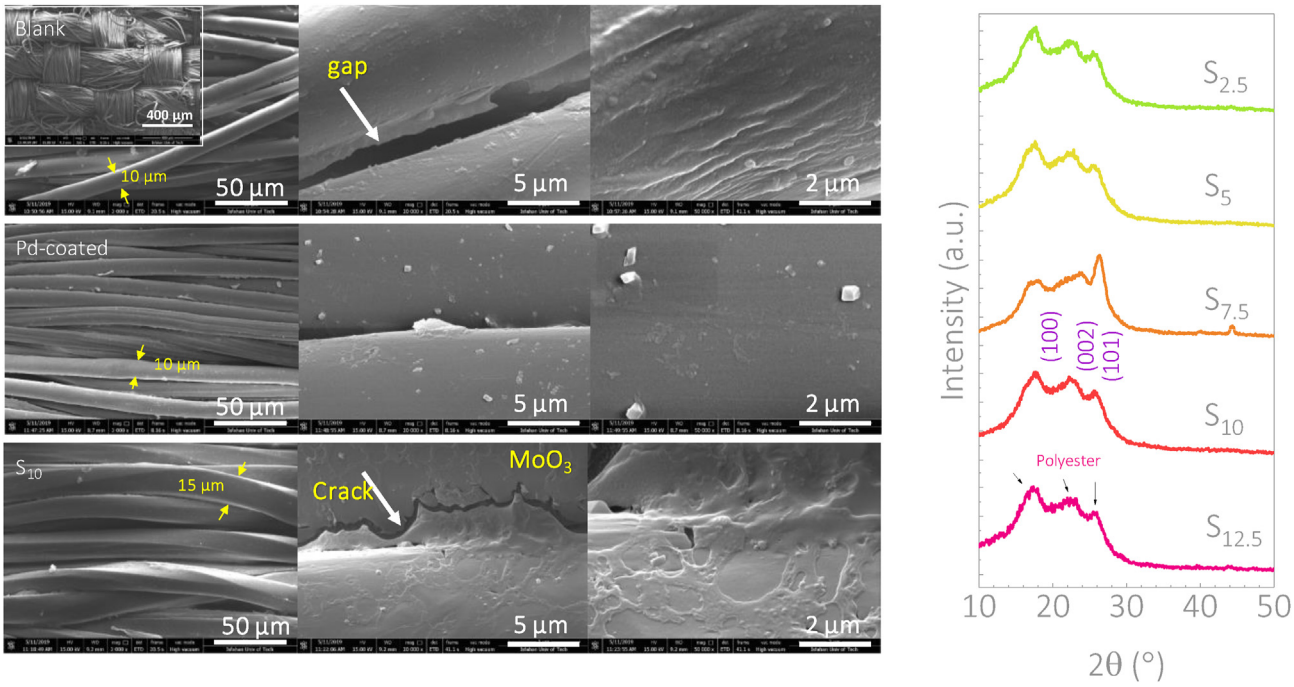

Fig. 2 – Left panel: FESEM images of different samples: blank polyester (the inside shows the overall texture), Pd-coated polyester fabric and after MoO_3 coating (sample S_{10}). Right panel: GIXRD pattern of different MoO_3 thin films on polyester fabrics which shows the amorphous nature of the layers.

Gasochromic properties

RGB investigations

This section provides a quantitative evaluation of the results of gasochromic investigation by the RGB module. RGB data were measured over time for each sample at different concentrations of hydrogen in the range of 250–10000 ppm (Fig. 3 left panel). The performance of hydrogen sensing can be described by total color differences (ΔC) equation defined according to the Euclidean distance [16]:

$$\Delta C = \sqrt{(\Delta R)^2 + (\Delta G)^2 + (\Delta B)^2} \quad (1)$$

where ΔR, ΔG and ΔB are changes in R, G and B data from the initial values, respectively (see Fig. 1(b)). For all the samples, ΔC increases rapidly with hydrogen exposure until it reaches a maximum value as hydrogen is replaced with air, then it decreases toward the background. The peak values of ΔC vary depending upon the hydrogen concentration. The maximum amount of ΔC values measured in each cycle are plotted as a function of hydrogen concentration in Fig. 3 right panel. All the plots appear to be well compatible with a linear function, which demonstrates the capability of the RGB module for gasochromic sensing of hydrogen in a wide concentration range and with a reliable process of calibration. Previous studies on gasochromic molybdenum oxide mainly focused on the optical properties change and, to our best knowledge, less attempts to provide a linear calibration curves have been reported for gas sensing applications. Interestingly, the slopes of the linear plots are almost the same for all samples, indicating a proper reproducibility of the sample responses regardless of the oxygen fraction in the deposition process of the RF sputtering. It is also worth noting that compared to the color difference (Eq. (1)), other values like the changes in mean values of RGB led to nonlinear calibration curves (not shown here). M. H. Yaacob et al. obtained a nonlinear concentration dependence (in the range of less than 0.06–1%) for the gasochromic molybdenum oxide layer deposited on quartz substrates. They did not show sufficient sensitivity at concentrations above 0.5% [51]. This could be due to the effect of the substrate type on the sensitivity.

UV–vis spectra

In this study, UV–Vis reflectance spectra were recorded to compare the RGB readout and optical spectral variations. Fig. 4(a) shows the reflection spectra of the gasochromic fabrics before and after hydrogenation with 10% H_2. The shoulder visible at about 400 nm could be related to the optical absorption edge of MoO_3. The spectra show uniform absorption for wavelengths above 450 nm. The total reflectance of the deposited samples before hydrogenation is calculated by integration in the range of 400–700 nm and plotted in terms of oxygen percentage (Fig. 4(b)), indicating a maximum at 7.5% O_2. Compared to the high magnification FESEM images taken from the surface of the coated monofibers (shown in the same figure), the higher reflectance may be due to the fact that sample $S_{7.5}$ has a smoother microstructure surface than the others. After hydrogenation, the reflectance decreases in all wavelength ranges, while the spectral shape remains almost identical to that before gas exposure, indicating a relatively neutral optical change. Fig. 4(c) shows the difference in the reflectance spectra before and after the gasochromic process.

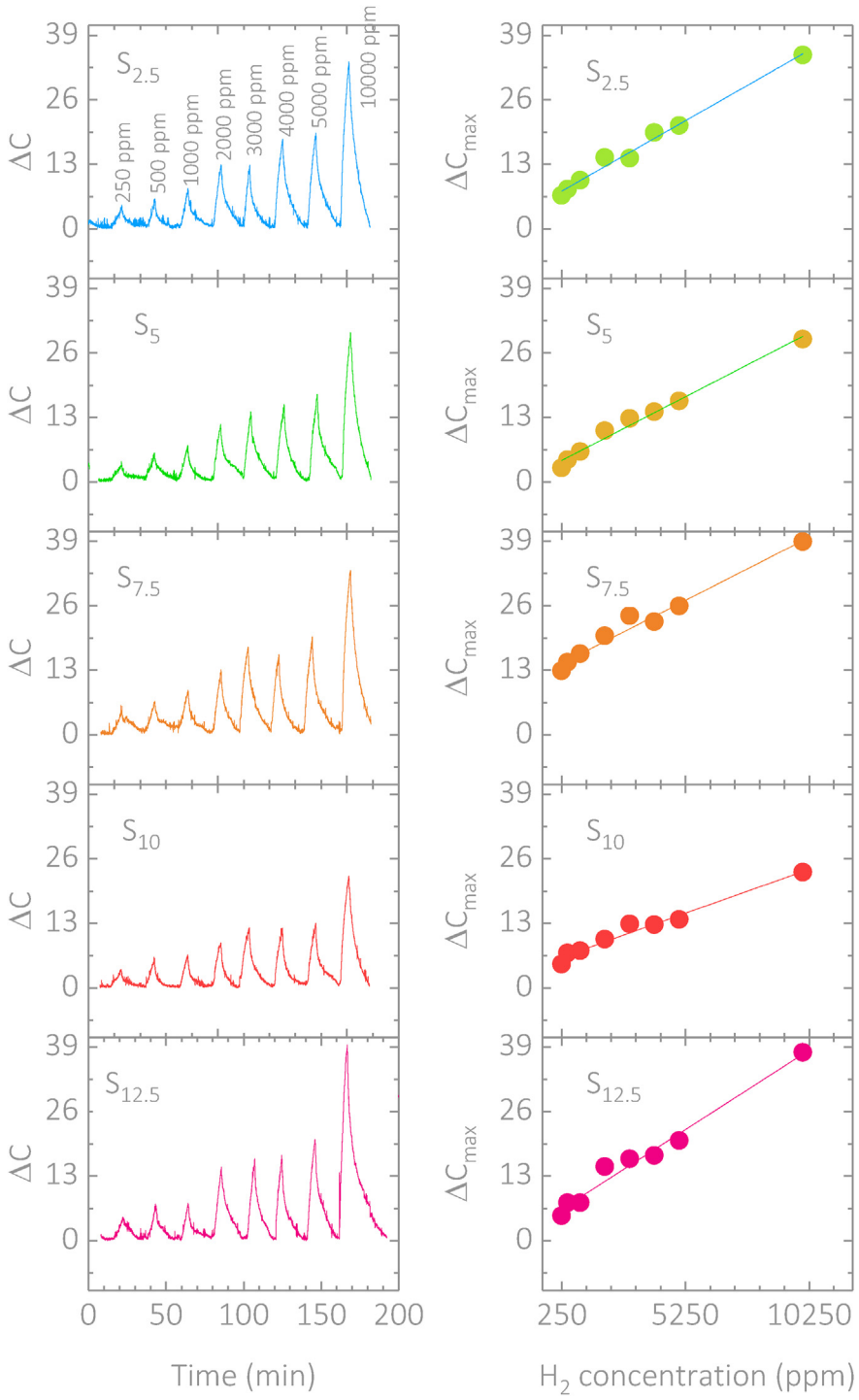

Fig. 3 – Left: Time variations of the total coloration differences (ΔCs) collected at different concentrations of hydrogen from 250-10000 ppm for samples $S_{2.5}$-$S_{12.5}$. The concentration of exposed hydrogen gas is the same for the same cycles in each sample. Right: corresponding plots of maximum ΔC vs. hydrogen concentration, which fit well to linear function.

The uniform decrease in reflectance over the entire 400–700 nm range is consistent with the relatively uniform changes in the RGB data (Fig. 3).

To compare the RGB and optical absorption data, the total absorption change (integration over 400–700 nm) was obtained. Fig. 4(d) shows ΔC (at 10,000 ppm) and total reflectance changes with respect to sputtering oxygen content. Although no specific trend is observed with increasing oxygen content, it behaves similarly for both quantities, indicating a correlation between RGB and optical reflectance data.

Another point to note is the increase in both at 12.5% O_2, which may be related to the role of oxygen in the formation of new oxygen vacancies in the molybdenum oxide layers. The oxygen concentration in the layers deposited by sputtering

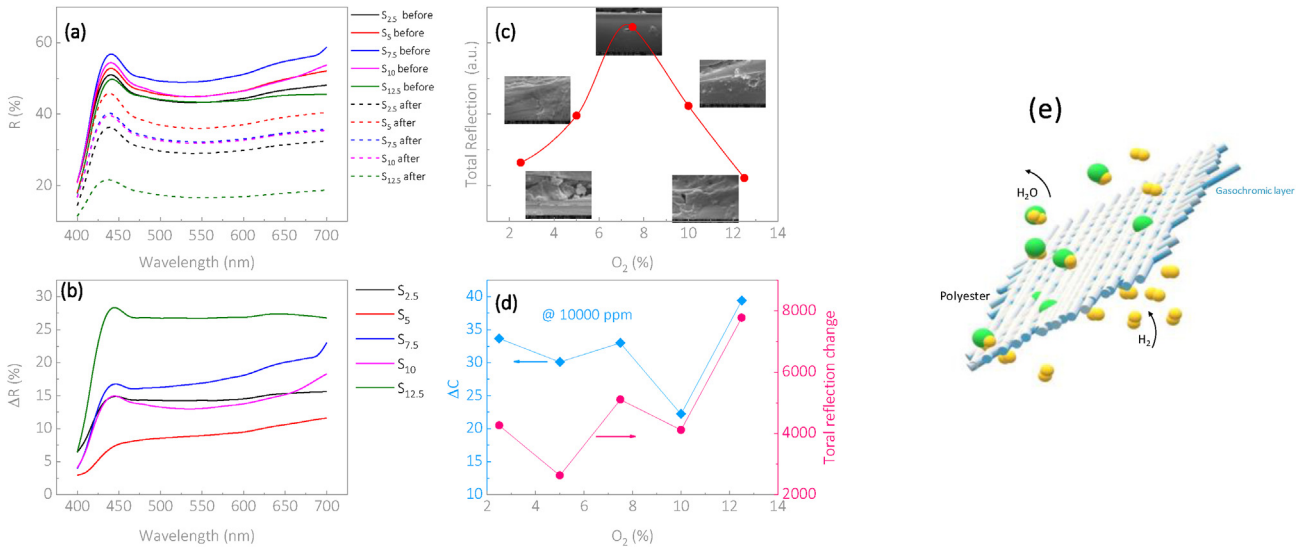

Fig. 4 – (a) UV–vis reflection of samples before and after 10% H_2 exposure at room temperature. (b) Total reflectance of as-prepared samples before hydrogen exposure. (c) Difference reflection (ΔR) and (d) ΔC at 10,000 ppm (from Fig. 3) and total reflectance change integral in terms of O_2 percent. (e) Schematic representation of water formation and highly desorption.

strongly depends on the fraction of reactive O_2 [52]. As a result of hydrogen diffusion in the gasochromic process, the generated H^+ species tend to combine with the bound oxygen in the oxide layer and form oxygen vacancies. The initial doping level of vacancies in oxygen-rich Mo oxide films (prepared in an oxygen-rich environment) is negligible, which increases rapidly with hydrogenation, and enhanced optical change is observed. Using XPS analyses, we have previously shown that a higher W^{5+}/W^{6+} ratio is associated with oxygen vacancies, which can lead to poor gasochromic performance in tungsten vanadium oxide films [53].

The color change of MoO_3 might be related to the formation of Mo^{5+} as suggested by previous studies [54]. The general coloration mechanism is related to hydrogen dissociation by a catalyst layer, more commonly Pd. The hydrogen donates its electrons to the conduction band and produces oxygen vacancy and Mo^{5+} states. The underlying mechanism is believed to be as follows:

$$\begin{aligned} &H_2 \xrightarrow{Pd} 2H^+ + 2e^- \\ &Mo^{6+} + e^- \rightarrow Mo^{5+} \\ &2H^+ + O^{2-} \rightarrow H_2O \end{aligned} \quad (2)$$

as a result of hydrogen intercalation into the molybdenum oxide lattice, the intervalence-charge transfer from Mo^{5+} to Mo^{6+} state occurs and a blue color is obtained by optical absorption in the NIR region. It is assumed that the optical absorption achieved is proportional to the Mo^{5+} concentration [55]. This suggests that ΔC is proportional to the concentration of Mo^{5+} and thus to the doped hydrogen. This is probably why the calibration curves show a linear behavior. Oxide gasochromic materials often suffer from irreversibility and repeatability [22,56]. It is believed that proton diffusion also gives rise to water molecules, which can slow down the coloration through blocking the pores [57]. The interaction of hydrogen with molybdenum oxide is reversible, but the unwanted formation of water slows this reversibility. This is also true to some extent for tungsten oxide [58]. This could be due to the entrapment of water molecules between the van der Waals layers of molybdenum oxide. Because compared to tungsten oxide, molybdenum oxide has a great tendency to layer structure due to the presence of van der Waals bonds between the crystallographic layers. However, this may be useful for interaction of small hydrogen molecules through diffusion across the layer. The open structure of polyester fabrics in addition to its hydrophobicity provide a large surface area and many open pathways for water desorption from the back uncoated surface (Fig. 4(e)), resulting in the reversibility and sensitivity of our samples. The MoO_3/Pd configuration does not decrease the reactivity due to limited exposure of Pd to H_2. A possibility for this system is that since hydrogen can penetrate the polymers, it is possible for hydrogen to reach the palladium layer from the polymer and enter the molybdenum oxide layer after decomposition. We do not have enough experimental evidence for this, but since many articles have shown that hydrogen can penetrate the polymer, this can be considered as a potential cause [25].

Coloration times

The gasochromic response time can be defined as the time required for the samples to reach 90% of the maximum changes. Similarly, the recovery time is the time required to return to 10% of background during recovery. However, this measurement is only useful when the sensor is saturated, which is not measurable in our case. However, if we use the maximum values of ΔCs, we can predict the effect of gas concentration on coloration rate. Inside Fig. 5(a), one can see how response and recovery times are measured for a typical sample.

Fig. 5(a and b) show the response time (t_{res}) and recovery time (t_{rec}), respectively, as a function of hydrogen concen-

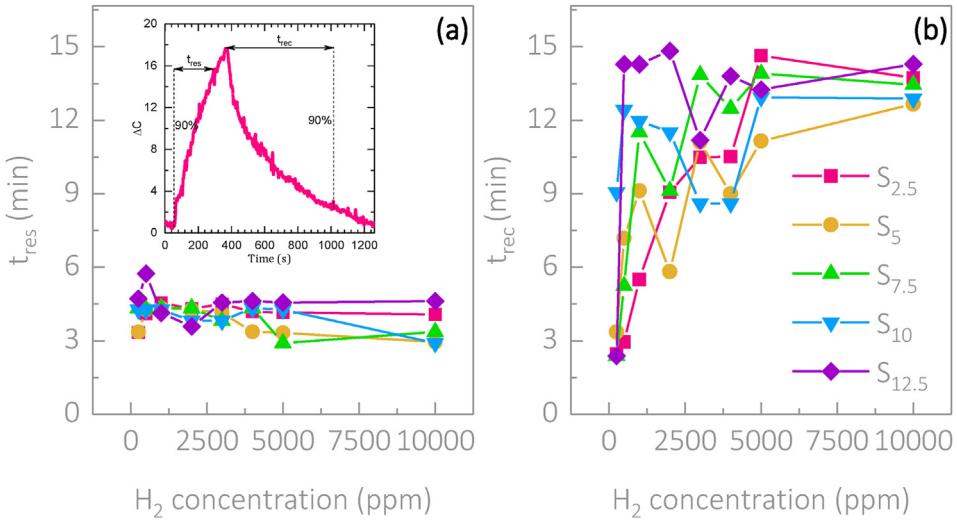

Fig. 5 – (a) Response and (b) recovery time plots as a function of hydrogen concentration. Inside part (a) shows how response and recovery times are obtained.

tration for all samples. From the figure, it can be seen that the response time for all samples and at all hydrogen concentrations is about 4 min. Although the recovery time depends on the hydrogen concentration, the same trend is observed for all deposition oxygen percentages. The recovery time at 250 ppm is about 1–3 min for most samples, which increases to about 14 min as the hydrogen concentration increases. However, a comparison of the recovery times in samples $S_{2.5}$ and $S_{12.5}$ indicates that it takes longer for the higher oxygen content (sample $S_{12.5}$) to compensate for the amount of oxygen lost during the gasochromic process. It should be noted that the response times should be better in the seconds range to approach the existing standards for a sensor. We have discussed this problem with filtration paper based sensors [59], but this case needs further investigation and optimization. This values are better compared to other reported gasochromic MoO3 films. Ch. Ch. Chang et al. have exposed molybdenum oxide films prepared by pulsed laser deposition on glass substrates with a thickness of about 1 μm to 100% hydrogen gas concentration and obtained coloration times of 12 min [60]. The shorter response times in our work can be attributed to the nature and porosity of the polyester substrates. However, they also reported a revocert time of about 17 min. Z. Zhang et al. [61] have shown that in Pd-doped sol-gel derived WO_3–MoO_3 composite films with a high ratios of WO_3, the sensor response is less than 1 min, but with increasing the percentage of MoO3 by about 50% or more, the response and recovery time increases considerably to about 1000 s. This predicta that molybdenum oxide and tungsten oxide composite films on polyester fabrics can even improve its response and reversibility, which will be considered in our future studies. However, MoO_3 room temperature optical hydrogen sensors still have slower response speed comparing to resistive based MoO_3 sensors [62]. This may be due to the fact that the electrical resistance has a linear relation to thickness but the optical properties have an exponential dependence.

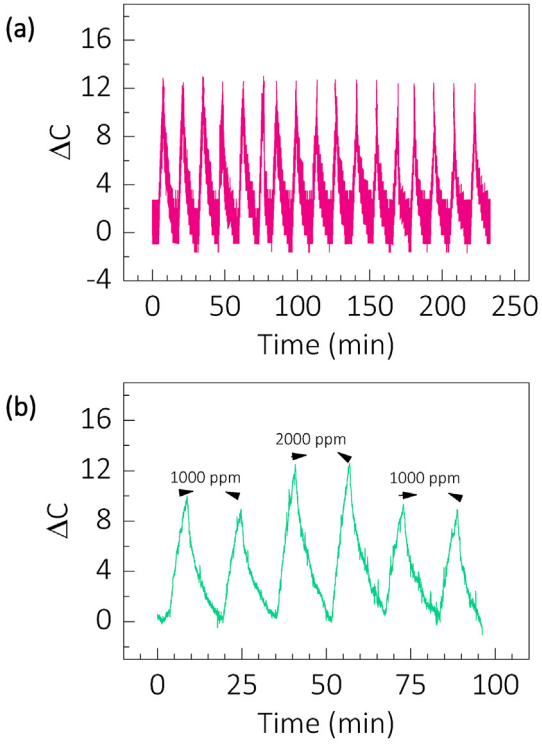

Fig. 6 – (a) The stability test of sample $S_{2.5}$ with 2500 ppm hydrogen gas. (b) The reproducibility test of this sample with 1000 and 2000 ppm hydrogen concentrations.

Stability

Fig. 6(a) shows the stability test of a typical sample ($S_{2.5}$) for 17 consecutive cycles. The sample was exposed to 2500 ppm hydrogen gas for 180 s per cycle followed by 600 s of air exposure. These results show that the sensor has good stability during cyclic gas measurement operation. Fig. 6(b) shows the coloring reproductive ability for this sample, which was

performed at two different concentrations of 1000 and 2000 ppm and at similar times to the stability test. The results of the measurements show the ability of the sensor to reliably reproduce the response to different concentrations of hydrogen gas. We tested stability at room temperature and constant humidity. During our tests, we found that over long time, the performance of the sensors may be somewhat reduced.

Conclusion

In summary, gasochromic polyester fabrics with linear sensitivity to hydrogen concentration and good reversibility and reproducibility were presented. Using DC and RF magnetron sputtering methods, Pd and MoO_3 layers (at different O_2/Ar ratio) were deposited on polyester fabrics. In the presence of hydrogen gas, the color of MoO_3/Pd/polyester changed, which could be well detected by an RGB color sensor module. The porous morphology of polyester fabrics remained after coating, which may allow increased hydrogen adsorption. It was found that although the oxygen content affects the optical/color change and response speed and recovery during RF sputtering of MoO_3, the linear sensitivity to hydrogen concentration is maintained, indicating that the sputtering method is desirable for the preparation of reliable samples. The desirable reversibility in the samples was attributed to the fibrous nature of the polyester substrate, which can repel the generated water molecules faster. The RGB data also showed good correlation with the optical data, promising the commercialization of flexible colorimetric hydrogen sensors.

Declaration of competing interest

The authors declare that they have no known competing financial interests or personal relationships that could have appeared to influence the work reported in this paper.

Acknowledgment

The authors would like to thank the Iranian National Science Foundation (INSF) for their financial support and also Department of Textile Engineering, Isfahan University of Technology for UV–Vis analysis.

Appendix A. Supplementary data

Supplementary data to this article can be found online at https://doi.org/10.1016/j.ijhydene.2021.09.195.

REFERENCES

[1] Dawood F, Anda M, Shafiullah GM. Hydrogen production for energy: an overview. Int J Hydrogen Energy 2020:3847–69. https://doi.org/10.1016/j.ijhydene.2019.12.059.

[2] Anikina ID, Sergeyev VV, Amosov NT, Luchko MG. Use of heat pumps in turbogenerator hydrogen cooling systems at thermal power plant. Int J Hydrogen Energy 2017;42:636–42. https://doi.org/10.1016/j.ijhydene.2016.04.256.

[3] Rochlitz L, Steinberger M, Oechsner R, Weber A, Schmitz S, Schillinger K, et al. Second use or recycling of hydrogen waste gas from the semiconductor industry - economic analysis and technical demonstration of possible pathways. Int J Hydrogen Energy 2019;44:17168–84. https://doi.org/10.1016/j.ijhydene.2019.05.009.

[4] Muradov N. Hydrogen via methane decomposition: an application for decarbonization of fossil fuels. Int J Hydrogen Energy 2001;26:1165–75. https://doi.org/10.1016/S0360-3199(01)00073-8.

[5] Tang J, Sheng Chu M, Li F, Feng C, Gen Liu Z, Sheng Zhou Y. Development and progress on hydrogen metallurgy. Int J Miner Metall Mater 2020;27:713–23. https://doi.org/10.1007/s12613-020-2021-4.

[6] Hübert T, Boon-Brett L, Black G, Banach U. Hydrogen sensors – a review. Sensor Actuator B Chem 2011;157:329–52. https://doi.org/10.1016/j.snb.2011.04.070.

[7] Wang B, Zhu LF, Yang YH, Xu NS, Yang GW. Fabrication of a SnO 2 nanowire gas sensor and sensor performance for hydrogen. J Phys Chem C 2008;112:6643–7. https://doi.org/10.1021/jp8003147.

[8] Martin L. Electrochemical hydrogen sensor for safety monitoring. Solid State Ionics 2004;175:527–30. https://doi.org/10.1016/j.ssi.2004.04.042.

[9] Korotcenkov G, Han S Do, Stetter JR. Sensors PH. Korotcenkov 2009.Pdf. 2009. p. 1402–33.

[10] Zhang Y nan, Peng H, Qian X, Zhang Y, An G, Zhao Y. Recent advancements in optical fiber hydrogen sensors. Sensor Actuator B Chem 2017;244:393–416. https://doi.org/10.1016/j.snb.2017.01.004.

[11] Herkert E, Sterl F, Strohfeldt N, Walter R, Giessen H. Low-cost hydrogen sensor in the ppm range with purely optical readout. ACS Sens 2020;5:978–83. https://doi.org/10.1021/acssensors.9b02314.

[12] Hwang SH, Kim YK, Jeong SM, Choi C, Son KY, Lee SK, et al. Wearable colorimetric sensing fiber based on polyacrylonitrile with PdO@ZnO hybrids for the application of detecting H2 leakage. Textil Res J 2020:2198–211. https://doi.org/10.1177/0040517520912729. 004051752091272.

[13] Wadell C, Syrenova S, Langhammer C. Nanoplasmonic hydrogen sensing. Plasmonics: Metallic nanostructures and their optical properties XII9163; 2014. p. 916310. https://doi.org/10.1117/12.2063399.

[14] Tripicchio P, Satler M, Dabisias G, Ruffaldi E, Avizzano CA. Towards smart farming and sustainable agriculture with drones. In: Proc - 2015 Int Conf Intell Environ IE. 2015; 2015. p. 140–3. https://doi.org/10.1109/IE.2015.29.

[15] Rouast PV, Adam MTP, Chiong R, Cornforth D, Lux E. Remote heart rate measurement using low-cost RGB face video: a technical literature review. Front Comput Sci 2018;12:858–72. https://doi.org/10.1007/s11704-016-6243-6.

[16] Greenawald LA, Boss GR, Snyder JL, Reeder A, Bell S. Development of an inexpensive RGB color sensor for the detection of hydrogen cyanide gas. ACS Sens 2017;2:1458–66. https://doi.org/10.1021/acssensors.7b00396.

[17] Fatoni A, Aziz AN, Anggraeni MD. Low-cost and real-time color detector developments for glucose biosensor. Sens Bio Sens Res 2020;28:100325. https://doi.org/10.1016/j.sbsr.2020.100325.

[18] Wittwer V, Datz M, Ell J, Georg A, Graf W, Walze G. Gasochromic windows. Sol Energy Mater Sol Cells 2004;84:305–14. https://doi.org/10.1016/j.solmat.2004.01.040.

[19] Deb SK. Opportunities and challenges in science and technology of WO3 for electrochromic and related

applications. Sol Energy Mater Sol Cells 2008;92:245–58. https://doi.org/10.1016/j.solmat.2007.01.026.
[20] Gogova D, Thomas LK, Camin B. Comparative study of gasochromic and electrochromic effect in thermally evaporated tungsten oxide thin films. Thin Solid Films 2009;517:3326–31. https://doi.org/10.1016/j.tsf.2008.12.020.
[21] Han S-I, Lee SY, Duy LT, Seo H. Reversible gasochromic hydrogen sensing of mixed-phase MoO3 with multi-layered Pt/Ni/Pt catalyst. Int J Hydrogen Energy 2021:33339–48. https://doi.org/10.1016/j.ijhydene.2021.07.091.
[22] Kalanur SS, Yoo IH, Seo H. Pd on MoO3 nanoplates as small-polaron-resonant eye-readable gasochromic and electrical hydrogen sensor. Sensor Actuator B Chem 2017;247:357–65. https://doi.org/10.1016/j.snb.2017.03.033.
[23] Yaacob MH, Yu J, Latham K, Kalantar-zadeh K, Wlodarski W. Optical hydrogen sensing properties of nanostructured Pd/MoO 3 films. Sens Lett 2011;9:16–20. https://doi.org/10.1166/sl.2011.1410.
[24] Chang C-C, Luo J-Y, Chen T-K, Yeh K-W, Huang T-W, Hsu C-H, et al. Pulsed laser deposition of (MoO3)1−x(V2O5)x thin films: preparation, characterization and gasochromic studies. Thin Solid Films 2010;519:1552–7. https://doi.org/10.1016/j.tsf.2010.09.003.
[25] You K, Cao F, Wu G, Zhao P, Huang H, Wang Z, et al. Room-temperature H 2 gasochromic behavior of Pd-modified MoO 3 nanowire labels. Mater Chem Phys 2019;227:111–6. https://doi.org/10.1016/j.matchemphys.2019.01.070.
[26] Rutherford JJ. Wearable Technology. IEEE Eng Med Biol Mag 2010;29:19–24. https://doi.org/10.1109/MEMB.2010.936550.
[27] Patel S, Park H, Bonato P, Chan L, Rodgers M. A review of wearable sensors and systems with application in rehabilitation. J NeuroEng Rehabil 2012;9:21. https://doi.org/10.1186/1743-0003-9-21.
[28] Hoang AT, Cho YB, Park J-S, Yang Y, Kim YS. Sensitive naked-eye detection of gaseous ammonia based on dye-impregnated nanoporous polyacrylonitrile mats. Sensor Actuator B Chem 2016;230:250–9. https://doi.org/10.1016/j.snb.2016.02.058.
[29] Siciliano T, Tepore A, Filippo E, Micocci G, Tepore M. Characteristics of molybdenum trioxide nanobelts prepared by thermal evaporation technique. Mater Chem Phys 2009:687–91. https://doi.org/10.1016/j.matchemphys.2008.10.018.
[30] Sunu SS, Prabhu E, Jayaraman V, Gnanasekar KI, Gnanasekaran T. Gas sensing properties of PLD made MoO3 films. Sensor Actuator B Chem 2003;94:189–96. https://doi.org/10.1016/S0925-4005(03)00342-3.
[31] Gesheva K, Szekeres A, Ivanova T. Optical properties of chemical vapor deposited thin films of molybdenum and tungsten based metal oxides. Sol Energy Mater Sol Cells 2003;76:563–76. https://doi.org/10.1016/S0927-0248(02)00267-2.
[32] Prasad AK, Kubinski DJ, Gouma PI. Comparison of sol–gel and ion beam deposited MoO3 thin film gas sensors for selective ammonia detection. Sensor Actuator B Chem 2003;93:25–30. https://doi.org/10.1016/S0925-4005(03)00336-8.
[33] Ali F, Khoshsirat N, Duffin JL, Wang H, Ostrikov K, Bell JM, et al. Prospects of e-beam evaporated molybdenum oxide as a hole transport layer for perovskite solar cells. J Appl Phys 2017;122:123105. https://doi.org/10.1063/1.4996784.
[34] Pérez-González M, Morales-Luna M, Santoyo-Salazar J, Crotte-Ledesma H, García-Tinoco PE, Tomás SA. Improved adsorption and photocatalytic removal of methylene blue by MoO3 thin films: role of the sputtering power, film thickness, and sputtering working pressure. Catal Today 2021;360:138–46. https://doi.org/10.1016/j.cattod.2019.06.003.
[35] Greene JE. Review Article: tracing the recorded history of thin-film sputter deposition: from the 1800s to 2017. J Vac Sci Technol A Vacuum, Surfaces, Film 2017;35:05C204. https://doi.org/10.1116/1.4998940.
[36] Favier F, Walter EC, Zach MP, Benter T, Penner RM. Hydrogen sensors and switches from electrodeposited palladium mesowire arrays. Science (80-) 2001;293:2227–31. https://doi.org/10.1126/science.1063189.
[37] Al-Mufachi NA, Rees NV, Steinberger-Wilkens R. Hydrogen selective membranes: a review of palladium-based dense metal membranes. Renew Sustain Energy Rev 2015:540–51. https://doi.org/10.1016/j.rser.2015.03.026.
[38] Shi J, Wu G, Shen J, Gao G, Zhou B, Ni X, et al. Preparation of Pd doped WO 3 films via sol-gel method and their gasochromic properties. Sixth Int Conf Thin Film Phys Appl, 2008:69843A. https://doi.org/10.1117/12.792153.
[39] Chan C-C, Hsu W-C, Chang C-C, Hsu C-S. Hydrogen incorporation in gasochromic coloration of sol–gel WO3 thin films. Sensor Actuator B Chem 2011;157:504–9. https://doi.org/10.1016/j.snb.2011.05.008.
[40] Kalhori H, Ranjbar M, Farrokhpour H, Salamati H. Fabrication of Pd/WO 3 colloidal nanoparticles by laser ablation in liquid of tungsten for optical hydrogen detection. J Laser Appl 2019;31:32018. https://doi.org/10.2351/1.5110352.
[41] Shafieyan AR, Ranjbar M, Kameli P. Localized surface plasmon resonance H_2 detection by MoO_3 colloidal nanoparticles fabricated by the flame synthesis method. Int J Hydrogen Energy 2019;44. https://doi.org/10.1016/j.ijhydene.2019.05.171.
[42] Zamharir SG, Ranjbar M, Salamati H. Excimer laser treatment of TiO2/WO3 thin films for self-cleaning gasochromic applications: preparation and characterization. Sol Energy Mater Sol Cells 2014;130:27–35. https://doi.org/10.1016/j.solmat.2014.06.029.
[43] Aray A, Ranjbar M. SPR-based fiber optic sensor using IMO thin film: towards wide wavelength tunability from visible to NIR. IEEE Sensor J 2019;19. https://doi.org/10.1109/JSEN.2018.2888509.
[44] Tavakoli Foroushani F, Tavanai H, Ranjbar M, Bahrami H. Fabrication of tungsten oxide nanofibers via electrospinning for gasochromic hydrogen detection. Sensor Actuator B Chem 2018;268:319–27. https://doi.org/10.1016/j.snb.2018.04.120.
[45] Shahzamani Z, Ranjbar M, Comini E, Goodarzi MT, Salamati H, Sberveglieri G. Palladium thin films on microfiber filtration paper as flexible substrate and its hydrogen gas sensing mechanism. Int J Hydrogen Energy 2019;44. https://doi.org/10.1016/j.ijhydene.2019.04.277.
[46] Ahmadi M, Tavanai H, Ranjbar M, Goodarzi MT. Hydrogen detection properties of palladium sputtered polyacrylonitrile nanofibrous layers. Polym Adv Technol 2021;32:1763–73. https://doi.org/10.1002/pat.5212.
[47] Kamel MM, El Zawahry MM, Helmy H, Eid MA. Improvements in the dyeability of polyester fabrics by atmospheric pressure oxygen plasma treatment. J Text Inst 2011;102:220–31. https://doi.org/10.1080/00405001003672366.
[48] Imawan C, Steffes H, Solzbacher F, Obermeier E. A new preparation method for sputtered MoO3 multilayers for the application in gas sensors. Sensor Actuator B Chem 2001;78:119–25. https://doi.org/10.1016/S0925-4005(01)00801-2.
[49] Nishizawa K, Yamada Y, Yoshimura K. Low-temperature chemical fabrication of Pt-WO3 gasochromic switchable films using UV irradiation. Sol Energy Mater Sol Cells 2017;170:21–6. https://doi.org/10.1016/j.solmat.2017.05.058.

[50] Lu Y-R, Hsu H-H, Chen J-L, Chang H-W, Chen C-L, Chou W-C, et al. Atomic and electronic aspects of the coloration mechanism of gasochromic Pt/Mo-modified V 2 O 5 smart films: an in situ X-ray spectroscopic study. Phys Chem Chem Phys 2016;18:5203–10. https://doi.org/10.1039/C5CP06870C.
[51] Yaacob MH, Yu J, Latham K, Kalantar-Zadeh K, Wlodarski W. Optical hydrogen sensing properties of nanostructured Pd/MoO3 films. Sens Lett 2011:16–20. https://doi.org/10.1166/sl.2011.1410.
[52] Oka N, Watanabe H, Sato Y, Yamaguchi H, Ito N, Tsuji H, et al. Study on MoO3−x films deposited by reactive sputtering for organic light-emitting diodes. J Vac Sci Technol A Vacuum, Surfaces, Film 2010;28:886–9. https://doi.org/10.1116/1.3328822.
[53] Ranjbar M, Mahdavi SMM, Iraji zad A. Pulsed laser deposition of W-V-O composite films: preparation, characterization and gasochromic studies. Sol Energy Mater Sol Cells 2008;92:878–83. https://doi.org/10.1016/j.solmat.2008.02.018.
[54] Fleisch TH, Zajac GW, Schreiner JO, Mains GJ. An XPS study of the UV photoreduction of transition and noble metal oxides. Appl Surf Sci 1986;26:488–97. https://doi.org/10.1016/0169-4332(86)90120-0.
[55] Rouhani M, Foo YL, Hobley J, Pan J, Subramanian GS, Yu X, et al. Photochromism of amorphous molybdenum oxide films with different initial Mo 5+ relative concentrations. Appl Surf Sci 2013;273:150–8. https://doi.org/10.1016/j.apsusc.2013.01.218.
[56] Borgschulte A, Sambalova O, Delmelle R, Jenatsch S, Hany R, Nüesch F. Hydrogen reduction of molybdenum oxide at room temperature. Sci Rep 2017;7:40761. https://doi.org/10.1038/srep40761.
[57] Georg A. The role of water in gasochromic WO3 films. Thin Solid Films 2001;384:269–75. https://doi.org/10.1016/S0040-6090(00)01865-4.
[58] Borgschulte A, Sambalova O, Delmelle R, Jenatsch S, Hany R, Nüesch F. Hydrogen reduction of molybdenum oxide at room temperature. Sci Rep 2017;7:1–9. https://doi.org/10.1038/srep40761.
[59] Shahzamani Z, Ranjbar M, Comini E, Goodarzi MTTMT, Salamati H, Sberveglieri G. Palladium thin films on microfiber filtration paper as flexible substrate and its hydrogen gas sensing mechanism. Int J Hydrogen Energy 2019;44:17185–94. https://doi.org/10.1016/j.ijhydene.2019.04.277.
[60] Chang CC, Luo JY, Chen TK, Yeh KW, Huang TW, Hsu CH, et al. Pulsed laser deposition of (MoO3)1 - X(V 2O5)x thin films: preparation, characterization and gasochromic studies. Thin Solid Films 2010;519:1552–7. https://doi.org/10.1016/j.tsf.2010.09.003.
[61] Zhang Z, Wu G, Gao G, Feng W, Jin X, Shen J. Structural study of WO3 and MoO3 compound films in H2 gasochromism. Key Eng Mater 2013:184–8. https://doi.org/10.4028/www.scientific.net/KEM.537.184.
[62] Yang P, Li X, Huang H, Yang S, Zhang X, Hu Y, et al. Hydrogen sensing kinetics of laterally aligned MoO3 nanoribbon arrays with accelerated response and recovery performances at room temperature. Int J Hydrogen Energy 2020;45:23841–50. https://doi.org/10.1016/j.ijhydene.2020.06.074.